The Korean Journal of Ceramics, **7**[1] 36-40 (2001)

Micromachinng and Fabrication of Thin Filmes for MEMS-infrarad Detectors

Sang-Seop Yom, Heung-Woo Park, Yun-Kwon Park, Byeong-Kwon Ju, Young-Jei Oh, Jong-Hoon Lee, Moonkyo Chung, Sang-Hee Suh and Geun Chang Hoang*†

Electronic Materials and Device Research Center, Korea Institute of Science and Technology, Seoul, 136-791, Korea
**Division of Physics, Wonkwang Univ., Iksan, Chonbuk, 570-749, Korea*

(Received September 23, 1998 · Accepted January 10, 2001)

In order to fabricate uncooled IR sensors for pyroelectric applications, multilayered thin films of $Pt/PbTiO_3/Pt/Ti/Si_3N_4/SiO_2/Si$ and thermally isolating membrane structures of square-shaped/cantilevers-shaped microstructures were prepared. Cavity was also fabricated via direct silicon wafer bonding and etching technique. Metallic Pt layer was deposited by ion beam sputtering while $PbTiO_3$ thin films were prepared by sol-gel technique. Micromachining technology was used to fabricate microstructured-membrane detectors. In order to avoid a difficulty of etching active layers, silicon-nitride membrane structure was fabricated through the direct bonding and etching of the silicon wafer. Although multilayered thin film deposition and device fabrications were processed independently, these could be integrated to make IR micro-sensor devices.

Key words: Uncooled IR sensor, MEMS, Multilayered thin film

I. Introduction

IR sensing technology has many applications utilizing contactless and nondestructive sensing of remote images.[1-4] Conventional IR detectors usually adopt semiconducting HgCdTe and InSb materials for 3~12 μm wavelength range. Although excellent performance of the semiconducting detector performance is realized, device cooling down to liquid nitrogen temperature is a huddle to make the detector convenient to field usage. To avoid the cooling problems, there are many types of uncooled IR detectors utilizing non-semiconducting materials: for example, resistive bolometers, pyroelectric detectors, and thermoelectric detectors. For the uncooled detectors, excessive local heating can generate electric current which causes bad performance of the sensors. So thermally well insulated active materials are required for that of high performance. One of the best solutions is to hybrid active material components onto membrane structures via silicon micromachining technique so-called MEMS.[5-7]

Pyroelectric device is known as a fast response and wide spectral range operation. One of the popular pyroelectric sensor materials is lead-titanate ($PbTiO_3$) which has large pyroelectic coefficient (γ=9.5 $\times 10^{-8}$ C/cm^2 K), large dielectric constant (ε=200), and other excellent physical properties.[8] Other researchers used thin films of perovskite $Ba_{1-x}Sr_xTiO_3$(BST) and $PbTi_{1-x}Zr_xO_3$(PZT) which are well known thin film materials for dynamic random access memory (DRAM) and ferroelectric random access memory (FRAM) applications. Unlike DRAM and FRAM application, improvement of the thermal isolation is required for the uncooled IR sensor technology. Fabrication of multilayered thin films is essential to operate better device performance. However, well oriented films of perovskite oxide material onto silicon followed by metallic platinum deposition are not easy to produce due to poor interfacial properties via high oxidation tendency during the device processing. In this work, we attempt to fabricate square-shaped, cantilevers-shaped, and cavity embedded back-etched suspending membrane structures[9-10] using a combination of surface micromachining and silicon wafer bonding technique. Preliminary study of the active element on the suspending structure showed photoresponse which is good enough for the pyroelectric IR sensor operation.

†Corresponding author: gchoang@wonkwang.ac.kr

II. Experiment

Thermally oxidized SiO_2 layer of 1 μm was formed onto 4" p-type Si(100) wafer. After patterning for etching which is described below, silicon-nitride (Si_3N_4) layer of approximately 300 nm was deposited by plasma assisted chemical vapor deposition (PECVD). As a bottom electrode, platinum was deposited by ion beam sputtering. Ion beam voltage/current of 1000 V/25 mA induced sputtering of platinum target to deposit typically 1000 Å with a deposition rate of 30 Å/min. Since adhesion of the platinum onto the silicon-nitride film was poor, a buffer layer of titanium thickness of 4 nm was pre-deposited prior to the platinum layer. X-ray

diffraction (XRD) pattern, using the CuKα line of the as-grown Pt/Ti/Si_3N_4/SiO_2/Si, showed Pt(111) peaks. Surface and cross-sectional images were studied by scanning electron microscopy (SEM) and atomic force microscopy (AFM).

Pyroelectrically active material of the $PbTiO_3$ was deposited by sol-gel method. Mixture of titanium isopropoxide $Ti[OCH(CH_3)_2]_4$ and 2-methoxyethanol was add to acetylacetone (2,4-pentanedione) for sol preparation. Gel was prepared by adding lead acetate trihydrate [$Pb(CH_3CO_2)_2 \cdot 3H_2O$] to the sol with Nitric Acid (HNO_3) as a catalysis. Spin coating using photoresistor spinner (Headway Research Inc. USA) was carried out for several times until desired thickness of the $PbTiO_3$ under 30 min/ 4000 rpm was obtained. Final heat treatment was done in a tube furnace at 550°C for 30 minutes. Typical $PbTiO_3$ thickness was 1000 Å having perovskite structure confirmed by XRD.

For type-A(square-shaped) and type-B(cantilevers-shaped) structures, we used catalyzed EPW solutions which were the mixture of ethlenediamine, pyrocatechil, pyrazine, and water at 115°C. The EPW solution has different etching rate for silicon wafers having (111), (110), and (100) directions. After silicon-nitride layer deposition, photolithograpy was used to form opening of the etching hole followed by the reactive ion etching (RIE) in the flowing argon of 30 sccm and CHF_3 of 15 sccm. The final etching rate using the EPW solution was approximately 1.1 μm/min. For the cavity-formed-silicon wafer via direct bonding, KOH solution was used. The ratio of KOH to Water was 4 g: 100 mL at 80°C. The cavity was formed on one side of the silicon wafer after following the HNO_3 surface treatment. Two wafers, with/without the cavity, were bonded face-to-face in a clean room of class 100 followed by a heat treatment at 1100°C for 4 hours. Backside of the silicon substrate without cavity was etched out by the KOH solution to make a cavity embedded suspending structure. Top electrode of IR sensor was formed by thermally evaporated gold or silver.

III. Results and Discussion

Fig. 1 shows an XRD pattern of the $PbTiO_3$/Pt/Ti/Si. Perovskite phase was easily identified without preferred orientation due to the polycrystalline natures of the bottom

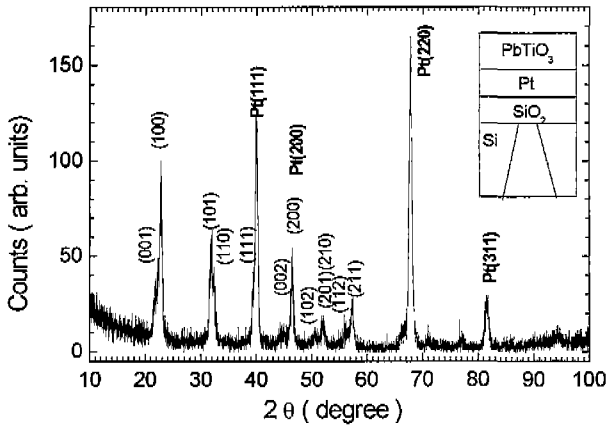

Fig. 1. XRD pattern of the $PbTiO_3$/Pt/Ti/Si.

electrodes. Compositional ratio of the $PbTiO_3$ was stochiometric which was confirmed by EPMA. Uncareful preparation of solution and poor heat treatment would result in unfavorable secondary phases. Peaks representing platinum bottom electrodes were also appeared in the XRD patterns.

Fig. 2 shows cross-sectional and surface SEM images of the $PbTiO_3$/Pt/Ti/Si_3N_4/SiO_2/Si. Bottom image shows surface of the $PbTiO_3$ layer indicating polycrystalline granular structure as expected from the XRD analysis. Cross-sectional SEM image shows configuration of multilayers of the $PbTiO_3$/Pt/Ti/Si_3N_4/SiO_2/Si. Thickness of each layer was easily distinguished from the cross-sectional SEM image. Some of the films after top electrode formation indicated high leakage current. Fig. 2 (A) and (B) have shown void formation between the $PbTiO_3$ and platinum due to a poor preparation of the surface during the cleaning process after deposition of the platinum. These voids were responsible for the fatal large leak current. We are currently under way to improve this processing step.

For MEMS based type-A(square-shaped) and type-B(cantilevers-shaped) structures, we designed masks for photolithograpy in order to make suspending structure shown in the top insert of Fig. 3. After formation of Si_3N_4/SiO_2/Si layers, photolithograpy was carried out followed by RIE. SEM images of type A indicated overhanging square shaped

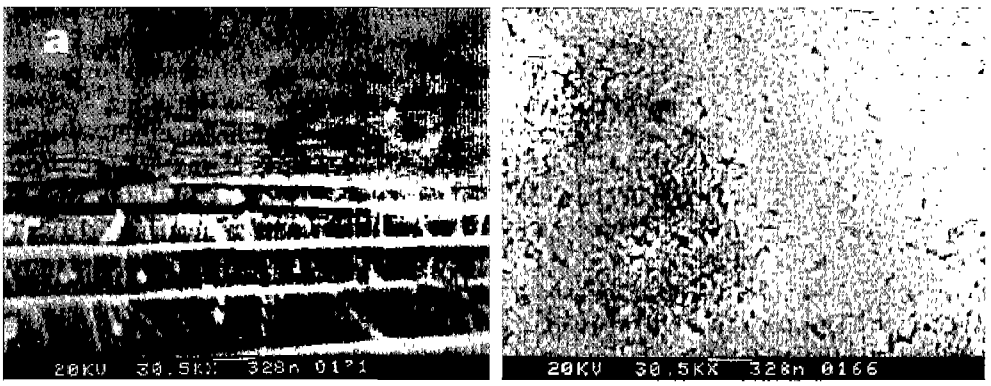

Fig. 2. (A) Cross-sectional and (B) surface SEM photographs of the $PbTiO_3$/Pt/Ti/Si_3N_4/SiO_2/Si.

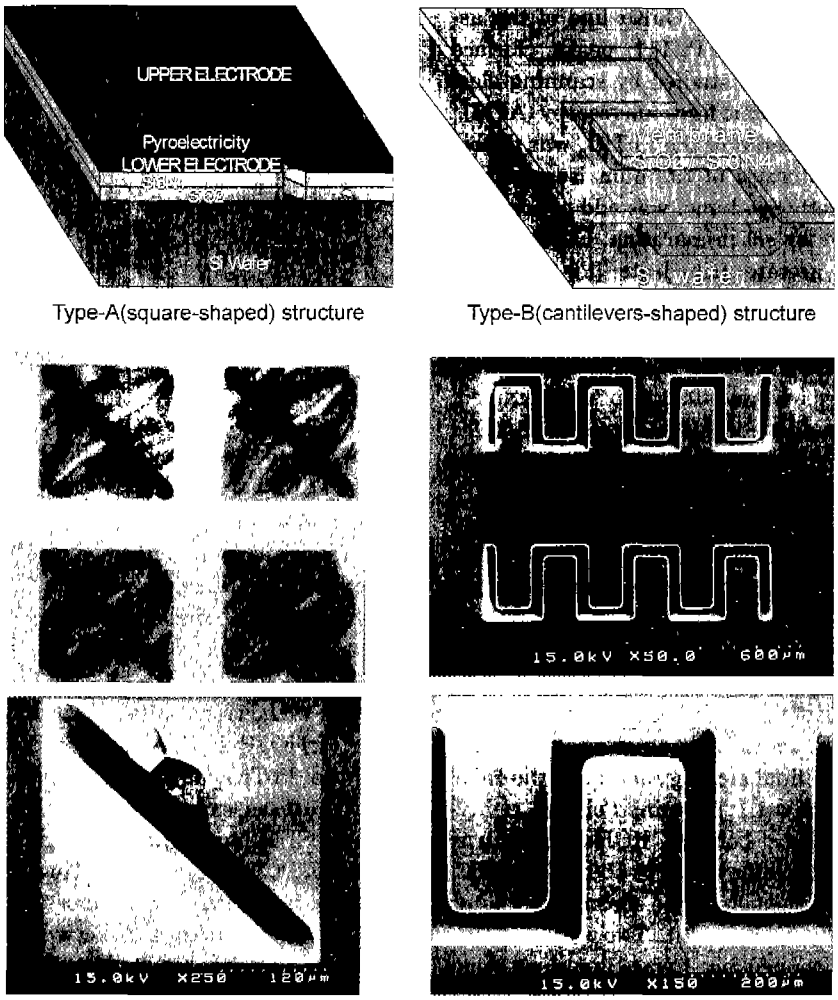

Fig. 3. Schematic diagram and SEM photographs of as-fabricated type-A(square-shaped) and type-B(cantilevers-shaped) structures.

structure. However, surfaces of the type A structure was not ideally flat due to chemical attack or stressed surfaces during the etching process. This can be improved by controlling etching time and other experimental parameters.

AFM images of inside/outside surfaces of overhanging square before/after the etching also indicated chemical attack. The type B structure did not experience severe chemical attack as compare with the type A structure. These structures may be very useful to make thermally isolated active element in MEMS based IR sensor array. Unfortunately, our technique of the sol-gel processing to deposit the $PbTiO_3$ was not compatible to making active layer after formation of the structures because chemical deposition method may have flatten out the structure. To avoid this difficulty, we attempted to build a cavity formed direct silicon wafer bonding structure, which can supply flat bottom electrodes surface for the sol-gel processing. It was successful to build a cavity formed direct silicon wafer bonding. However, bonding strength measured between the Si_3N_4 and SiO_2 was lower than that of direct silicon bonding.

Fig. 4 shows cross-sectional SEM image of the cavity formed silicon wafers. The top picture showed the cavity formed silicon wafer direct bonding structure. The middle one indicated the magnified bonding interface, which showed good layering scheme in sequence such as silicon substrate 1, thermally oxidized SiO_2 layer, silicon nitride layer, wafer bonded interface, silicon nitride, thermally oxidized SiO_2 layer, and substrate 2. There was no void formation during wafer bonding process. In order to obtain above mentioned flat bottom electrode surface, substrate 2 was back-etched using KOH solution. Thermally oxidized SiO_2 layer acted as an etching-stop-barrier during back-etching of the substrate 2. Bottom of Fig. 4 shows AFM photograph of the surface roughness of the silicon-nitride membrane after back-etching of the bonded structure. Square root mean square surface roughness was 1.6 Å with maxim hight difference of 16 Å, indicating smooth surface, which is good enough to fabricate thermally isolated MEMS based IR sensors.

We tried to deposit platinum and the $PbTiO_3$ layers onto the membrane structures for the IR sensor application. Some of the films were not good enough to make IR sensor

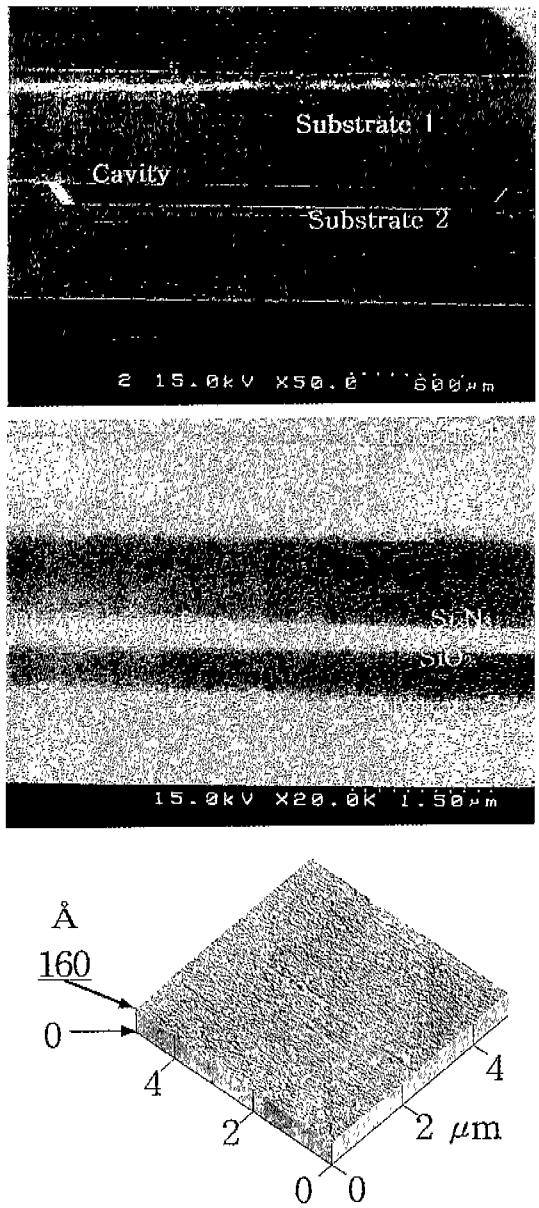

Fig. 4. (Top) Cross-sectional SEM photograph of the cavity formed silicon wafer direct bonded structure. (Middle) Magnified SEM photograph of the bonding interface of the bonded structure. (Bottom) AFM photograph of the surface roughness of the silicon-nitride membrane after back-etching of the bonded structure.

operation due to chemical attack during the complicated procedure. For example, void formation as mentioned above at the interface was fatal. We are currently working to improve the quality of the active layers. In order to demonstrate IR sensing operation, we fabricated simple Au/$PbTiO_3$/Pt/Ti/Si_3N_4/SiO_2/Si multilayered films without membrane structures and measured their photoresponse. The current versus bias voltage (I-V) curves were measured at room temperature in Fig. 5. They showed ohmic behavior. Photoresponse can be calculated from differential I-V curves. Poor signal of photoresponse was originated from

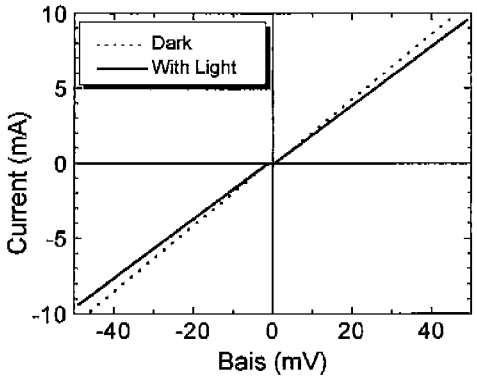

Fig. 5. Current versus bias voltage (I-V) curves of the $PbTiO_3$/Pt/Ti/Si without membrane structures. Photoresponse is to be calculated from differential I-V curves for room-light illumination.

the polycrystalline nature of the $PbTiO_3$ film, while better photoresponse was observed in the films grown on expensive single crystalline MgO or $SrTiO_3$ substrate in which micromachining technique is virtually impossible to apply.

IV. Summary and Conclusion

We have successfully prepared thermally isolating membrane structures of square-shaped/cantilevers-shaped microstructures and cavity formation via direct silicon wafer bonding and etching technique in order to fabricate uncooled infrared sensors for pyroelectric applications. Multilayered thin films of Pt/$PbTiO_3$/Pt/Ti/Si_3N_4/SiO_2/Si were prepared by PECVD, ion beam sputtering, sol-gel technique, sputtering, and thermal evaporation techniques. Photoresponse of multilayered films without membrane structures demonstrated possible IR sensor operation. Micromachining technology was powerful enough to isolate active pyroelectric sensor material from substrate. In order to obtain flat bottom electrodes surface for sol-gel process, it seems that our design of the cavity embedding direct silicon wafer bonding is very powerful. We are currently researching to improve device properties.

Acknowledgements

This work was supported by the Korea Institute of Science and Technology through the Ministry of Science and Technology. S. S. Yom supported in part by the Korea Science and Engineering Foundation through the Research Center of Dielectric and Advanced Matter Physics at Pusan National University.

References

1. P. W. Kruse, *Infrared Technology XXI*, SPIE 2552, 556 (1995).
2. P. W. Kruse, "Elements of Infrared Technology," Jon Wiley and Sons, NY(1962).

3. E. H. Putly, "Thermal Detectors," Spinger-Verlag (1977).
4. I. H. Choi, *IEEE Trans. On Electron Dev. ED-33*, 72 (1986).
5. M. Mescher, T. Abe, B. Brunett, H. Metla, T.E. Schlesinger and M. Reed, "Proceedings of IEEE-MEMS'95," (Amsterdam, Netherland, 261(1995).
6. J. P. Rice, *et al.*, SPIE 2159, 98 (1994).
7. D. L. Poola, *et al.*, *MRS Bulletin*, July 1996, 59 (1996)
8. J. J. Ho, Y. K. fang, K. H. Wu, W. T. Hsieh, C. W. Chu, C. R. Huang, M. S. Ju and C. P. Chang, *IEEE Electron Device Letters*, 19, 189 (1988) and references therein.
9. S. D. Senturia, "Mechanical Properties of Microelectronic Materials," in "Integrated Micro-Motion Systems Micromachining Control and Applications," Eds. F. Harashima, Elsilver Scien. Publ. 95-116 (1990).
10. N. Takeshima and H. Fujita, "Polyimide Bimorph Actuators for a Ciliary Motion System," 1991 ASME Winter Meeting, DSC-**Vol 32** (*Micromechanical Sensors, Actuators, and Systems*), 203-209.
11. Y. S. Yoon, D. H. Lee, T. S. Kim, M. H. Oh and S. S. Yom, *J. Vac. Sci. Technol. A*, **12**(3), 751 (1994).